Digest Journal of Nanomaterials and Biostructures Vol. 19, No. 4, October-December 2024, p. 1407-1418

Investigation of electrochemical performance of gadolinium trichloride in asymmetric supercapacitor applications

S. Shanmugha Soundare [a], S. Ariponnammal [b] , R. Jayavel [a,*]
[a]*Centre for Nanoscience and Technology, Anna University,Chennai-600 025, Tamilnadu, India*
[b]*Department of Physics, Gandhigram Rural Institute, Deemed To Be University, Gandhigram-624 302,Dindigul District, Tamilnadu, India*

The commercial Gadolinium tri chloride ($GdCl_3$) electrode material exhibits high specific capacitance of 207.52Fg^{-1} in three electrode system at 1A/g with potential window 1.0 V. The $GdCl_3$//Activated carbon (AC) asymmetric supercapacitor device in two electrode system achieves 188.14Fg^{-1} specific capacitance at 1 A/g with high potential window 1.7V. It possess high energy density 75.51Wh/kg, power density 850W/kg. and electrochemical stability of 92% of its initial capacitance after 5000 cycles. These demonstrate $GdCl_3$ as an useful material for electrochemical energy storage devices. Further, electron paramagnetic resonance study on $GdCl_3$ reveals g-factor 1.98 and line width ΔH = 221.8mT.

(Received July 23, 2024; Accepted October 4, 2024)

Keywords: $GdCl_3$, XRD, Cyclic voltammetry, Electrochemical impedance spectroscopy, EPR

1. Introduction

Energy crisis is one main issue that the technological and industrial sectors need to overcome. It seems more enticing to address this problem with supercapacitors. Technologically, advanced energy storage solutions for regulating supply and demand have included batteries and supercapacitors. Among them, supercapacitors are the best due to their higher power density, low maintenance costs, consistent charging, cost-effective energy density, rapid charge and discharge rates, and safety compared to ordinary capacitors. Low density energy and delayed kinetics of mass charge transfer are produced by bare electrodes. Therefore, they are not suitable for use in practical applications. Consequently, altering the electrode material is a useful strategy for raising the supercapacitor's efficiency and the operating mechanism depends on active material's performance [1]. So, researchers aimed to raise the energy density, surface area, and electrochemical capacitance. Rare earth nano particles have excellent electrochemical characteristics[2]. Multivalent rare earth compounds are a novel class of electrode material for supercapacitors. Due to their peculiar 4f electronic structure and high spin–orbit coupling, they display outstanding pseudocapacitive performance. Owing to their high bulk density and advantageous redox properties, rare earth based materials offer outstanding conductivity and are a good fit for creating supercapacitors. In this field, a variety of rare earth materials are used so far. A supercapacitor's excellent performance is mostly dependent on its enormous surface area, longer voltage stability, and higher electronic conductivity, as was previously mentioned. Through doping, rare earth elements largely contribute to surface area expansion and higher electrical conductivity in electrode materials[2]. It is interesting to note that gadolinium sulfide (Gd_2S_3) has a wide range of uses in energy storage, fuel cells, semiconductor technology, and electrocatalysis[3-4]. The electrolyte's electrical conductivity is reportedly increased by Gd^{3+}. This makes it perfect for applications involving energy storage[5]. For example, Gd_2S_3 rod-embedded RGO is a good choice for very sensitive electrochemical carbofuran detection, according to V. Mariyappan et al[6]. It has been demonstrated that Gd_2S_3 increases the stability of carbon-based composite materials as well as their surface area, porosities, conductivity, and

* Corresponding authors: rjvel@annauniv.edu
https://doi.org/10.15251/DJNB.2024.194.1407

electrocatalysis activity[1]. Gd doping, enhances electrochemical performance. The charge transfer resistance is reduced by Gd doping[7]. The production of oxygen vacancies in $Gd_xSr_{1-x}NiO_3$ results in an extraordinary increase in its electrochemical energy storage capacity. When x = 0.7 is substituted for Gadolinium in $SrNiO_3$, the result is an electrode with extraordinary activity. It has a recognizable voltage window and a noteworthy specific capacitance of $764Fg^{-1}$ in potassium hydroxide and $929Fg^{-1}$ in sodium sulfate. Furthermore, gadget has a remarkable power density $1kWkg^{-1}$ and energy density roughly $54Whkg^{-1}$ at $1Ag^{-1}$, and extraordinary large specific surface area[8]. Improved electrochemical performance for energy storage applications has been reported in Gadolinia based electrodes with high-conductivity nickel sulfide. It offers plenty of ions vacancies in electrochemical process with exceptional super capacitive nature[9]. For solid oxide fuel cells, Ceria doped with Gadolinium, $Ce_{0.85}Gd_{0.15}O_{1.5}$ cathode, was investigated at a moderate temperature[10-11]. Rare earth chlorides have been demonstrated to be efficient cathodic inhibitors[12]. The current work undertakes a comprehensive investigation of $GdCl_3$ in energy storage applications for future continuous power supply for charging electronic devices after taking the aforementioned points into account. The $GdCl_3$//Activated carbon (AC) asymmetric supercapacitor has been constructed using commercial manufactured Gadolinium tri chloride ($GdCl_3$) and the results of thorough electrochemical analysis has been presented in this paper. In addition, this work also examines $GdCl_3$ electron paramagnetic resonance studies.

2. Materials and methods

$GdCl_3$, a rare earth compound, is defined by x-ray powder diffraction (XRD) by PANalytical X'Pert Pro using Cu Kα radiation, electrochemical measurements by Bio-Logic VSP potentiostat model, and electron paramagnetic resonance (EPR) spectrum by Bruker model EMXplus spectrometer at room temperature.

$GdCl_3$ and activated carbon (AC) are two active materials. Using NMP solution (N-methyl pyrrolidone), active material, acetylene black, and binder material PVDF were combined to form an 85:10:5 paste. This slurry combination was then applied to $1cm^2$ of Ni foam, which was vacuum-dried for eight hours at 80°C.The coated substance has a mass of $2mg/cm^2$. The negative electrode in this experiment was 1x1 cm^2 AC electrode, and the positive electrode was $GdCl_3$. The specific capacitance of each unique active material was determined using the half-cell test, of three-electrode configuration. Ag/AgCl and platinum wire were utilized as reference and counter electrodes in three-electrode test, respectively, while 3M KOH served as the electrolyte. In a conventional three-electrode and two-electrode setup using 3M KOH electrolyte, the compositional advantages and favorable structural characteristics, as well as the electrochemical characteristics of $GdCl_3$ and activated carbon material on Nickel Foam (NF), were assessed.

3. Results and discussions

3.1. XRD

Hexagonal structure with lattice parameters[13] of a=b=7.363±0.01Å, c= 4.105±0.02Å, and V= 222.54 $Å^3$ is confirmed by $GdCl_3$ XRD, as shown in Figure 1. They agree with ASTM values that have been reported (JCPDS No:73-0482).

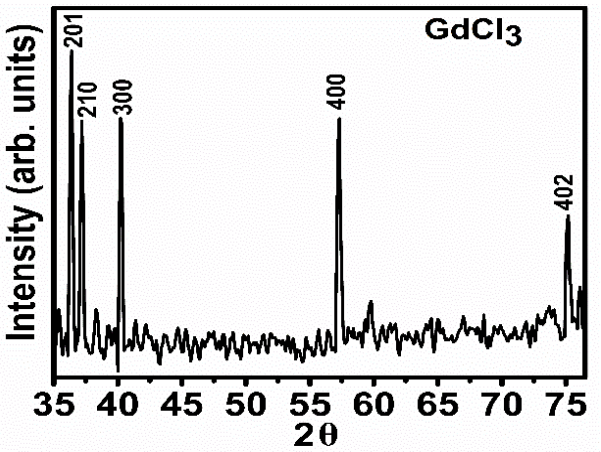

Fig. 1. XRD pattern of $GdCl_3$.

3.2. Electrochemical mechanism of $GdCl_3$ in alkaline electrolyte

A pseudo-capacitor is designed using water soluble commercial inorganic salts as electrode material in alkaline electrolyte. The electrochemical investigation based on ionic level is depicted in Fig.2. In pseudocapacitors of water-soluble inorganic salt, it has been noticed that reactive cations can transform into colloids. Strong specific capacitance can be attributed to these colloids' strong reactivity in electrochemical reaction.The function of Gd^{3+} in pseudocapacitors during the electrochemical redox reaction is discussed in this work. Coprecipitation and an external electric field helped to convert Gd^{3+} cations into GdOOH, which is more reactive to redox reactions. The current findings demonstrate that the electrochemical performance of $GdCl_3$ salt pseudocapacitors was significantly influenced by the crystallization kinetics. The understanding of the redox mechanism of active cations can be made further by the construction of ion-based pseudocapacitors. In the current reaction system, the alkaline electrolyte underwent simultaneous electrochemical redox reactions and crystallization. GdOOH molecules that were electrochemically reactive crystallized with the assistance of alkaline electrolytes and an external electric field[14]. Figure 2 depicts how $GdCl_3$ salts react with supercapacitor electrodes in alkaline electrolytes during electrochemical redox reactions.

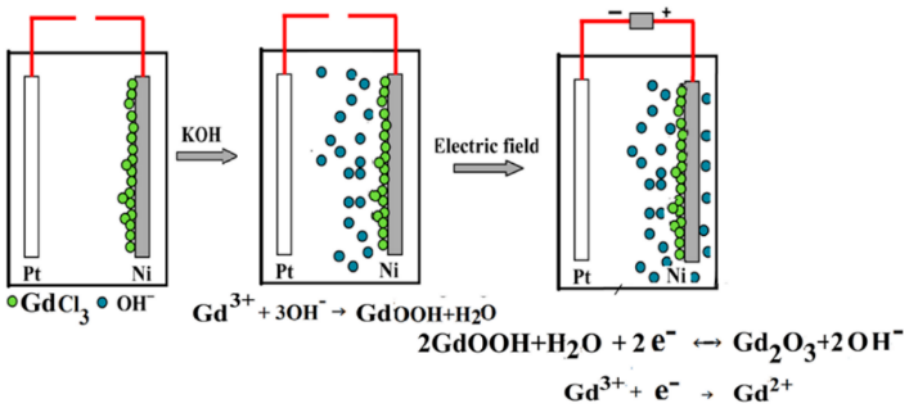

Fig. 2. Electrochemical mechanism of $GdCl_3$ in alkaline electrolyte.

Reactive materials with an uncommon reactivity toward pseudocapacitive reactions are formed more frequently when chemical coprecipitation and electrochemical processes are linked. After conducting an electrochemical test, we examined the phases and microstructures of the $GdCl_3$ salt electrodes in order to determine their reaction mechanism. The XRD patterns of the $GdCl_3$ salt electrodes following electrochemical characterization are displayed in Fig. 3.

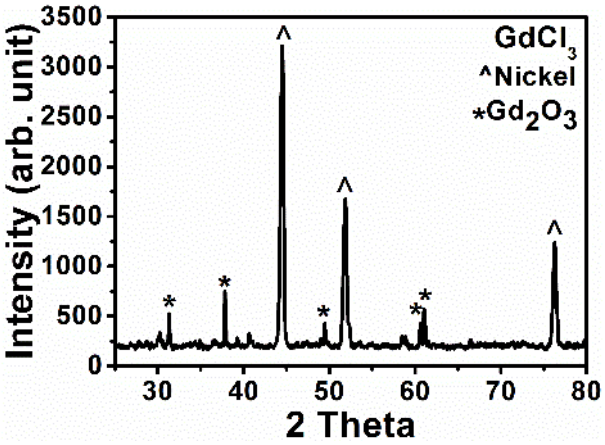

Fig. 3. XRD of $GdCl_3$ after electrochemical reaction in alkaline electrolyte.

It displays the XRD pattern of the blended electrodes, which include the binder, conductive carbon, and $GdCl_3$. The low intensity peak was attributed to Gd_2O_3 phase, with the exception of the Ni current collector peaks(JCPDS File No:87-0712). The subsequent response may transpire:

$$2GdOOH \div H_2O + 2e^- \rightarrow Gd_2O_3 + 2OH^-$$

$$Gd^{3+} + e^- \rightarrow Gd^{2+}$$

We produced the electrodes using only $GdCl_3$ in order to demonstrate the native role of these salts. The Gd_2O_3 phases were produced during electrochemical measurement, as demonstrated by the XRD pattern. The faint peaks suggested that the crystalline nature of the Gd_2O_3 colloids was not very good. The aforementioned findings verified that an alkaline electrolyte was the site of the chemical coprecipitation of Gd_2O_3 colloids[14]. The second dehydration breaks down $Gd(OH)_3$ into the intermediate GdOOH and finally into monoclinic Gd_2O_3 (JCPDS No.42-1465).

3.3. Electrochemical analysis on $GdCl_3$ by three electrodes system

Cyclic voltammetry(CV), Galvanostatic charging and discharging(GCD) and Electrochemical impedance spectroscopy (EIS) measurements have examined the supercapacitive (SC) characteristics connected to the $GdCl_3$ electrode. CV responses between -0.9 and 0.1V potential at 5, 10, 25, 50, 75, and 100 mV/s scan rates in 3M KOH aqueous electrolyte are depicted in Figure 4a.

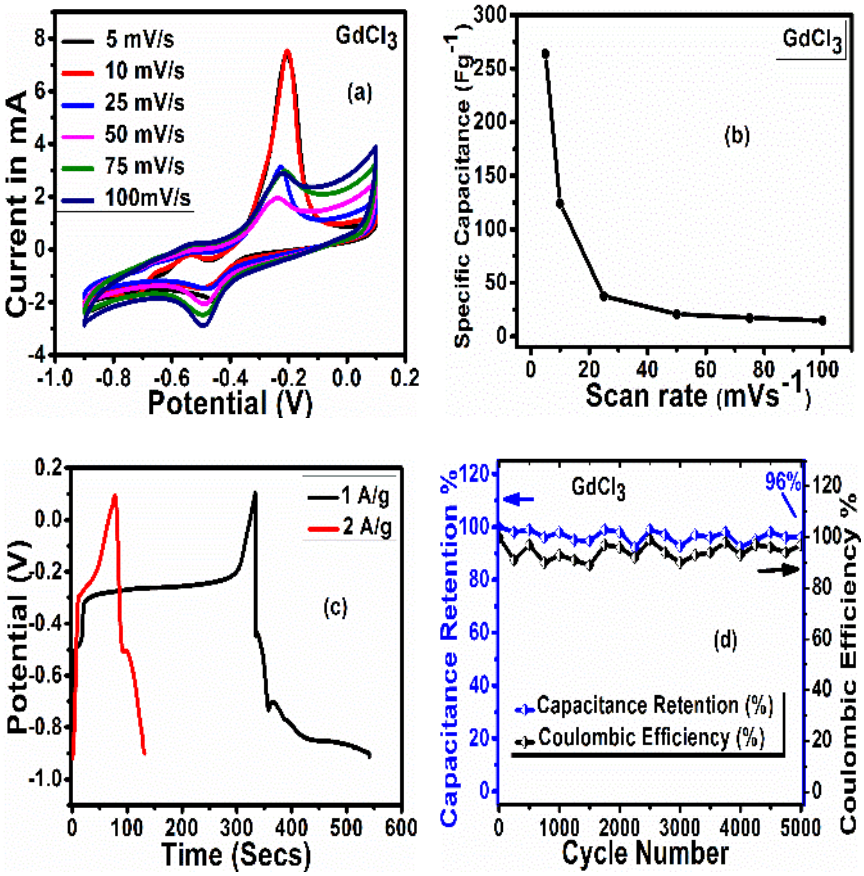

Fig. 4. (a) Cyclic voltammetry, (b) Specific capacitance versus scan rate, (c) GCD curves and (d)Cyclic stability of $GdCl_3$ three electrode system.

The operational potential window is 1V. CV plots (Figure 4a) of $GdCl_3$ exhibit a quasi-reversible faradic reaction that involves an electron transfer process concerning the enhanced charge storage, which is ascribed to the OH's ability to intercalate reversibly into a reduced form pseudo capacitance. As scan rate rises, as seen in Figure 4b, the area under the CV curve rises as well, which subsequently led to a specific capacitance drop corresponding to electrode-electrolyte interaction. At scan rates of 5, 10, 25, 50, 75, and 100 mV/s, specific capacitances of $GdCl_3$ are 263.77Fg^{-1}, 124.20Fg^{-1}, 37.54Fg^{-1}, 20.9Fg^{-1},17.33Fg^{-1}, and 14.67Fg^{-1}. Ions can access all sites at lower scan rates because they have sufficient time of diffusion to approach each active site in active electrode material, resulting high specific capacitance. On the other hand, due to the electrolyte's partial rate of transport, at higher scan rates, electrolyte ions are unable to diffuse all accessible locations of active electrode, resulting fall in specific capacitance[15]. Therefore, improved performance has an overall impact on $GdCl_3$[16].

The rare earth $GdCl_3$ electrode material shows one reduction peak at -0.45 V in cathode scan and two peaks of oxidation at -0.54 V and -0.20 V in anode scan. During the anode scan, the sample's Gd oxidation state shifts between Gd^{3+} and Gd^0 due to reversible conversion, made possible by faradic reactions[17]. Additionally, the well-maintained CV curve profiles show an increase from 5 to 100 mV/s scan rate, indicating that faradic reactions would likely exhibit outstanding electronic conductivity, excellent electrochemical reversibility, and quick ion/electron transfer kinetics. A redox signal is visible (Figure 4a) at greater scan rate 100 mV/s, suggesting effective charge transfer associated with adsorption behavior of ions OH^- in $GdCl_3$ electrode[16].

By measuring the materials' capacity to hold charges and analyzing the galvanostatic charge-discharge (GCD) patterns, a deeper understanding of the sample electrode's overall energy storage performance was attained. In Figure 4c, GCD curves are displayed. According to the GCD profile, the charge storage of $GdCl_3$ exhibits pseudocapacitive behavior as a result of Faradaic redox

reaction, which is consistent with the CV's findings. The remarkable coulombic efficiency of the $GdCl_3$ electrode was supported by electrode's GCD curves at 1 and 2 A/g current densities, which displayed a nearly symmetric charging and discharging time (Figure 4c). The $GdCl_3$ discharge curve (Figure 4c) has a kink because untransformed platform of Gd oxidation in process of reduction are missing at higher current densities[17]. GCD curves presented in Figure 4c for the $GdCl_3$ electrode exhibit near-symmetry, thereby verifying the superior electrode material quality of the sample and the flawless operation of a supercapacitor. Additionally, a calculation was performed to determine specific capacitance (Csp) change with current density (Figure 4c). Specific capacitance is 207.52 F/g at 1 A/g and 104.98 F/g at 2 A/g[18].

Electrochemical long-term cyclic stability of $GdCl_3$ electrode after several cycles of charging and discharging, was investigated. Figure 4d displays the capacitance retention curves for the $GdCl_3$ electrode as a function of GCD cycles. Electrode retained 96% of initial capacity even after 5000 GCD cycles at current density 3A/g from -0.9 to 0.1 V, indicating the stability of the material for prolonged use.

Impedance spectroscopy approach is quite reliable since it can manage wide range of resistances, capacitances, inductances, and obstructions presented by working electrode to alternating applied current. The Nyquist plot for $GdCl_3$ is shown in Figure 5 to help with the electron transport analysis.

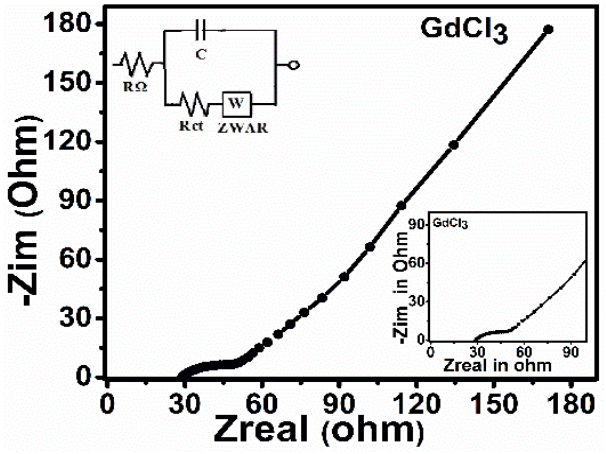

Fig. 5. Nyquist plot of $GdCl_3$.

Charge transfer resistance is indicated by one semicircle that has a series resistance of Rs 29.02 Ω and resistance of charge transfer 35.99 Ω[19]. Gd doping decreases the height and width of the Nyquist semicircle significantly[7].The Nyquist plot comparable circuit model is displayed as an inset in Figure 5. It can be used to explain processes at the electrode when kinetics and diffusion are not negligible. A double layer capacitor C, solution resistance (RΩ), and charge transfer resistance also known as the Warburg element, or ZWAR which provides species-specific diffusion coefficient information are all included in the Randles circuit, which is depicted as an inset in Figure 5. Under semi-infinite conditions, the Warburg impedance (Figure 5) depicts a straight line with a 45° slope[19]. In line with CV research, the impedance analysis circle illustrates the charge transfer resistance contribution.

3.4. Electrochemical analysis of activated carbon in three electrode system

After optimizing the positive electrode, a thorough electrochemical investigation was conducted on the activated carbon negative electrode. In the activated carbon (AC) electrode, electric double-layer serves as main energy storage system and beneficial for high power and long cycle life. Figure 6a shows the CV curve for the single AC-based negative electrode at distinct scan speeds from 0 to -1 V, ranging from 10 to 100 mV/s. The commercial AC electrode, which is formed like a rectangle,

has good qualities of electric double-layer capacitance. GCD curves with symmetrical and linear shapes show good reversibility. Based on the electrode's galvanostatic charge/discharge curve (Figure 6b) at 1 A/g, specific capacitance of AC-electrode was approximately 82.86 Fg^{-1}. These findings imply that the AC-based electrode can function as negative electrode in our asymmetric $GdCl_3$ based supercapacitor and can thus offer a sufficient capacitive performance[20].

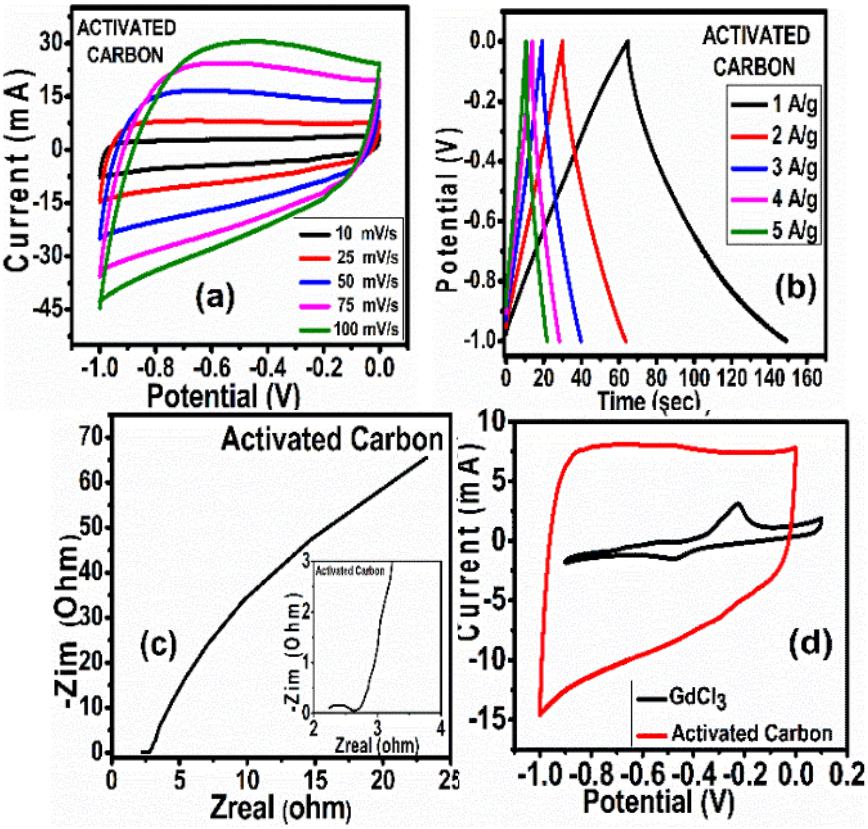

Fig. 6. (a) Cyclic voltammetry, (b)GCD curves, (c)Nyquist plot of activated carbon,and (d)Comparison of CV of $GdCl_3$ and activated carbon.

Nyquist plot of activated carbon is shown in Figure 6c. It shows one very small semicircle with a series resistance of Rs 2.244 Ω and a resistance of charge transfer as 0.410 Ω, indicating negligible charge transfer resistance[19]. The Warburg impedance represents a straight line with a 45° slope under semi-infinite conditions[19], which indicates a favorable supercapacitive nature. The CV of $GdCl_3$ and activated carbon has been compared in Figure 6d.

3.5. Construction of asymmetric (ASC) $GdCl_3$//AC supercapacitor

A manual press was used to compress the constructed $GdCl_3$ positive electrode and activated carbon negative electrode. For negative electrode, an AC/NF electrode piece was used, along with a polyurethane foam separator and a piece of $GdCl_3$/NF ($1\times1cm^2$) for the positive electrode. In the mean time, 3M KOH was used to soak the electrodes and separator for roughly two hours. Then, devices were constructed by placing a separator between the $GdCl_3$/NF and AC/NF electrodes. The charge balance theory improved mass balancing of positive and negative electrodes[21]. Teflon tape was utilized to accurately seal the manufactured devices to provide a dependable function. High rate capability of both positive and negative electrodes allowed us to create high-performing electrodes, which paved the way for the use of such innovative materials in consumer electronics. Consequently, constructed asymmetric capacitor may reach high energy and power density[22].

3.6. Electrochemical analysis asymmetric supercapacitor $GdCl_3$//AC

The $GdCl_3$/NF and AC/NF electrode's electrochemical performance has been evaluated at 25mV/s scan rate (Figure 6d) to determine ideal operating potential window -0.9 to 0.1 V and -1.0 to 0 V by three-electrode system. Then, an ASC was built to look into possible applications for the separate positive and negative electrodes. Because of three-electrode performance of each individual electrode, it was maintained during the ASC fabrication process that the mass ratio from positive to negative electrode was approximately 0.4. The produced ASC was limited to ≈1.7 V, the range for which the electrochemical analysis was carried out, as the oxygen evolution reaction started to appear beyond 1.7V.

Electrical conductivity, electrochemical reversibility, dominating charge storage mechanism, and relative contributions of all the charge storage mechanisms involved are only a few of the electrochemical characteristics that CV may assess for a given material. Figure 7a shows CV profiles of $GdCl_3$//AC electrode, which were acquired at six successively higher scan speeds between 5 and 100 mV/s. As seen in Figure 7a, cyclic voltammetry profiles covered a tiny area at 5mV/s and gradually grew when scan rate was increased to 100 mV/s. CV curves shape is almost rectangular. By comparing and contrasting actions related to charge storage at lower and higher scan rates, an energy storage device's rate performance demonstrates how strong it is. As scan speeds increase, quasi-symmetric and comparable CV curve morphologies are observed, demonstrating the electrode's high rate capabilities.

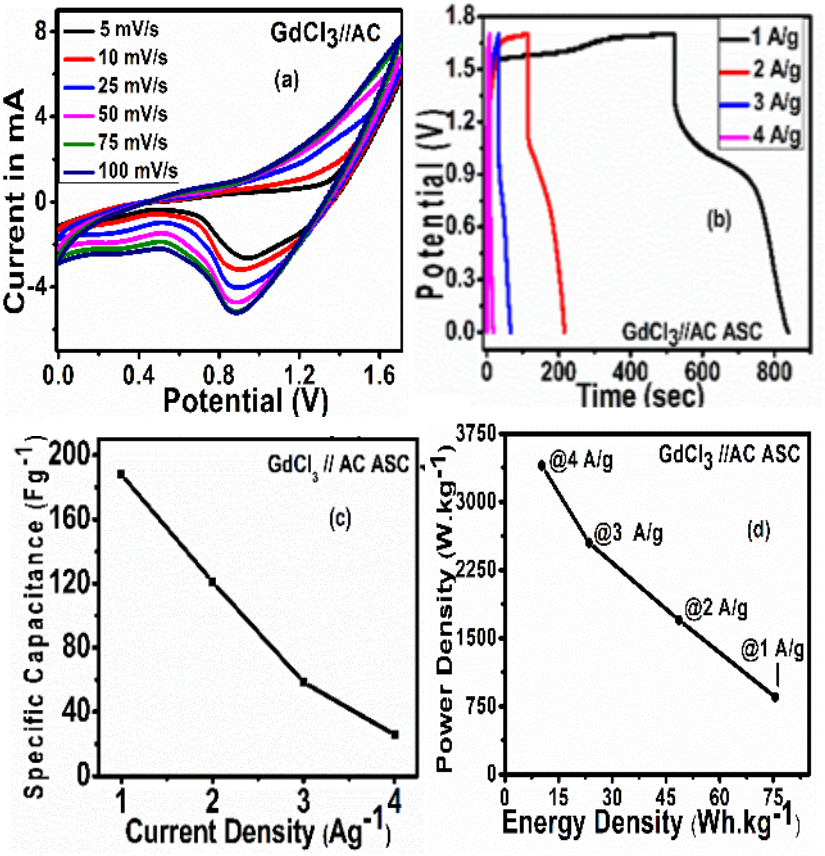

Fig. 7. (a) Cyclic voltammetry, (b) GCD curves, (c) Specific capacitance versus current density, and (d)Ragone's plot of $GdCl_3$ //AC asymmetric energy device of two electrode system.

Table 1. Results from GCD analysis of $GdCl_3$//AC ASC.

Current Density (A/g)	Specific Capacitance (F/g)	Energy Density (Wh kg^{-1})	Power Density (W kg^{-1})
1	188.14	75.51	850
2	121.06	48.59	1700
3	58.5128	23.48	2550
4	25.68	10.31	3400

The GCD curves shown in Figure 7b are essential for understanding SCs and evaluating the capacitors' real-world performance. GCD curves at current densities from 1 to 4 A/g of ASC revealed a close-symmetric nature within the 0 - 1.7 V potential window, indicating the continuity in the redox processes and their effectiveness at higher currents. GCD curves of asymmetric $GdCl_3$//AC are nonlinear due to pseudocapacitive nature of electrode-electrolyte interface, where electrochemical adsorption-desorption reactions take place. Based on estimates, the specific capacitance values at current densities 1A/g, 2A/g, 3A/g, and 4A/g are 188.14Fg^{-1}, 121.06Fg^{-1}, 58.51Fg^{-1}, and 25.688 Fg^{-1}, respectively (Figure 7c). There is a general tendency for capacity degradation with increased current density due to limitation of faradic redox processes at electrode surface and lower accessibility of incoming ions on electrode surface. Electrochemical capacitors have density of energy in proportion to the square of voltage across the cell. So, broader working potential window of an asymmetric device is principally responsible for its enhanced energy density. Table 1 shows operational parameters energy density (E) and power density (P) from galvanostatic curves. Ragone plot (Figure 7d) is a useful tool for evaluating the efficiency of electrochemical capacitors since it illustrates the link between energy density and power density. The ultimate energy density of $GdCl_3$//AC ASC is 75.51Wh/kg at 850W/kg power density, while maximum power density 3400W/kg may be sustained at energy density 10.31Wh/kg. Furthermore, generated electrode exhibits relatively little capacitance loss after extended endurance.

In case of cyclic stability, a longer electrochemical cycle life is a vital requirement of supercapacitor devices. Cyclic stability is depicted in Figure 8a. $GdCl_3$//AC asymmetric supercapacitor operating at 1.7 V was evaluated for its cycling performance using galvanostatic charge/discharge cycling at 3A/g for 5000 cycles. For the first 2000 cycles, there was a slight fluctuation in specific capacitance, or the electrode material's activation. Then, over the next 2000 cycles, specific capacitance progressively rises. After 5000 cycles, asymmetrical $GdCl_3$//AC device showed good coulombic efficiency and 92% retention.

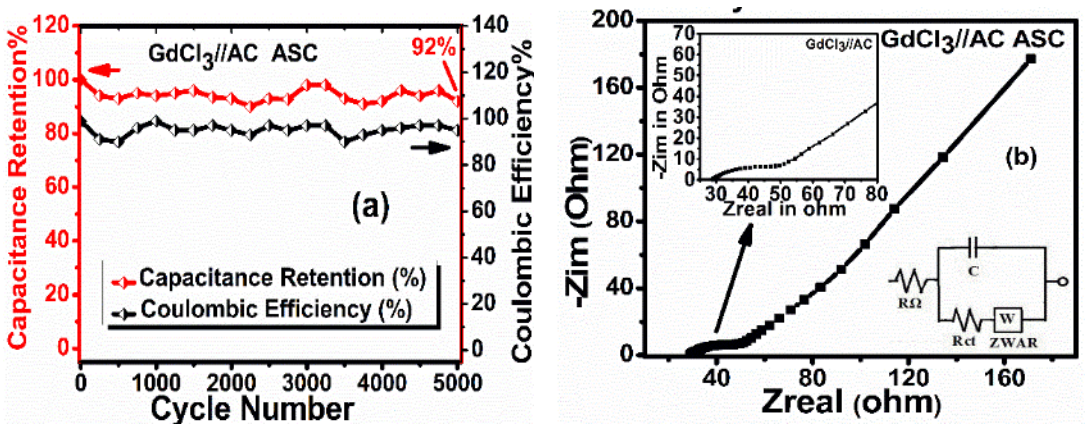

Fig. 8. (a) Cyclic stability and (b).Nyquist plot $GdCl_3$.

Nyquist plot of the asymmetric energy device $GdCl_3$//AC is displayed in Figure 8b. Charge transfer resistance is indicated by one semicircle that has a series resistance of Rs 29.57Ω and resistance of charge transfer 27.03Ω[19]. In semi-infinite conditions, the Warburg impedance is a straight line with a 45° slope[19]. In line with CV research, the impedance analysis circle illustrates the charge transfer resistance contribution.

3.7. Electron paramagnetic resonance

In Figure 9, the $GdCl_3$ EPR spectrum is shown. Gd^{3+}, the para-magnetic ion, has an electronic structure of $4f^7$. Ground state of Gd^{3+} ion is $^8S_{7/2}$. EPR spectrum is composed of these seven transitions ($\Delta M = \pm 1$). EPR investigations on S-state ions in host materials are great interest due to the characteristics crystal field exerted over ion and details discovered regarding mechanism causing ground state to zero field split. Among the four common S-state ions in EPR, Gd^{3+}, Eu^{2+}, Fe^{3+}, and Mn^{2+}, most insignificant hyperfine terms are present in the trivalent form of Gd^{3+} in a diamagnetic host. The zero orbital angular momentum of Gd^{3+} ion causes it to behave differently from other rare earth ions. Crystalline electric field affect only energy levels of gadolinium by high order interactions. As a result, spin-lattice relaxation period is quite long and the initial splitting of 8S levels is relatively small [23-25]. Conversely, the EPR spectrum (Figure 9) reveals a broad EPR line resonance with line width of ΔH = 221.8 mT and a g-factor of 1.98 at its center. The EPR line is broad and incredibly bright because of the high concentration of gadolinium present. Within the wide EPR line, all seven hyperfine lines are hidden.

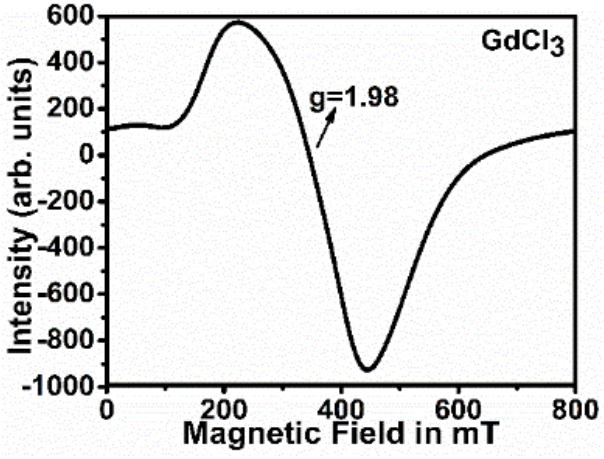

Fig. 9. EPR spectrum of $GdCl_3$.

4. Conclusions

The $GdCl_3$//Activated carbon (AC) asymmetric supercapacitor has been constructed using Gadolinium tri chloride ($GdCl_3$). The structure of gadolinium trivalent chloride is hexagonal. Using a 3M KOH electrolyte, electrochemical analysis has been performed using a traditional three-electrode and two-electrode configuration. The reported operational potential window in a three-electrode setup is 1V. The improved charge storage process through electron transfer is validated by the pseudocapacitance behavior displayed by CV. Between Gd^{3+} and Gd^0, the oxidation state of Gd changes. Pseudocapacitive behavior consistent with CV is confirmed by GCD. Even after 5000 cycles, cyclic stability still exhibits 96% of its initial capacity.

The contribution of charge transfer resistance is shown by impedance analysis. After the positive electrode was adjusted, an electrochemical investigation was performed on the activated carbon negative electrode. For high power and extended cycle life, it displays electric double-layer behaviour, which is in charge of the activated carbon electrode's fundamental energy storage mechanism. The Nyquist plot suggests a supercapacitive nature that is advantageous. A two electrode system asymmetric energy device with high rate capabilities was built using $GdCl_3$//AC. There is 1.7V potential window. The nature of ASC was close-symmetric. At an energy density

10.31 Wh/kg, highest power density 3400 W/kg is recorded. At power density 850W/kg, $GdCl_3$//AC ASC has energy density 75.51Wh/kg. It displays very low capacitance loss. High coulombic efficiency and 92% retention after 5000 cycles are features of asymmetric $GdCl_3$//AC. Coming to the real use, energy storage device's stability is an important factor. Furthermore, paramagnetic gadolinium's EPR spectrum reveals a large EPR line resonance with line width of ΔH = 221.8mT and g-factor of 1.98. The EPR line is broad and incredibly bright because of the high concentration of gadolinium present. Within the wide EPR line, all seven hyperfine lines are hidden.

Acknowledgments

Authors are thankful to SAIF-IITM, Chennai, India, for access to the EPR facility.

References

[1] Ponnaiah Sathish Kumar, Yuho Min, Dong Choon Hyun, Ji-Hyuk Choi, Sungwon Lee, J. Energy Storage **74**, 1098 (2023); https://doi.org/10.1016/j.est.2023.109385
[2] H.Huang, J.J.Zhu, Analyst **144**, 6789 (2019); https://doi.org/10.1039/C9AN01562K
[3] X.Rui, H.Tan, Q.Yan, Nanoscale **6**, 9889 (2014); https://doi.org/10.1039/C4NR03057E
[4] S.K.Ponnaiah, P.Prakash, Int. J. Hydrog. Energy **46**, 19323 (2021); https://doi.org/10.1016/j.ijhydene.2021.03.077
[5] H.M.Shiri, A.Ehsani, J. Colloid Interface Sci. **484**, 70 (2016); https://doi.org/10.1016/j.jcis.2016.08.075
[6] V.Mariyappan, M.Keerthi, S.M.Chen, J. Agric. Food Chem. **69**, 2679 (2021); https://doi.org/10.1021/acs.jafc.0c07522
[7] Muhammad Aadil, Anmar Ghanim Taki, Sonia Zulfiqar, Abdur Rahman, Muhammad Shahid, Muhammad Farooq Warsi, Zubair Ahmad, A.Asma, Alothman, Saikh Mohammad, RSC Adv. **13**, 28063 (2023); https://doi.org/10.1039/D3RA05290G
[8] M.I.A.Abdel Maksoud, Ramy Amer Fahim, Ahmed Esmail Shalan, M.Abd Elkodous, Olojede, S.O.Ahmed, I.Osman, Charlie Farrell, H.Ala'a, A.S.Al-Muhtaseb Awed, A.H.Ashour, W.David, Rooney, Environ. Chem. Lett. **19**, 375 (2021); https://doi.org/10.1007/s10311-020-01075-w
[9] S.Dhanalakshmi, A. Mathi Vathani, V.Muthuraj, N.Prithivikumaran, S.Karuthapandian, J. Mater. Sci. Mater. Electron. **31**, 3119 (2020); https://doi.org/10.1007/s10854-020-02858-1
[10] Arif Nazir, Fraz Khalid, Shafiq ur Rehman, Masood Sarwar, Munawar Iqbal, Muhammad Yaseen, Muhammad Iftikhar Khan, Mazhar Abbas, Z .Phys. Chem. **235**, 745 (2021); https://doi.org/10.1515/zpch-2019-1473
[11] Bibi, Ismat, Hussain, Sabir, Majid, Farzana, Kamal, Shagufta, Ata, Sadia, Sultan, Misbah, Din, Muhammad Imran, Iqbal, Munawar, Nazir, Arif, Z. Phys. Chem. **233**, 1431(2019); https://doi.org/10.1515/zpch-2018-1162
[12] Ajit Kumar Mishra, R.Balasubramaniam, Mater. Chem. Phys. **103**, 385 (2007); https://doi.org/10.1016/j.matchemphys.2007.02.079
[13] C.Au, R.Au, Acta. Cryst. **23,** 1112 (1967); https://doi.org/10.1107/S0365110X67004426
[14] Byung-II Lee, Heejin Jeong, Jung-soo Bae, Song-Ho Byeon, Chem. Commun., **49, 6051** 2013); https://doi.org/10.1039/C3CC42760A
[15] Kalimuthu Vijaya Sankar, D.Kalpana, Ramakrishnan Kalai Selvan, J. Appl. Electrochem. **42**, 463 (2012); https://doi.org/10.1007/s10800-012-0424-2
[16] Rashmirekha Samal, Barsha Dash, Chinmaya Kumar Sarangi, Kali Sanjay, Tondepu Subbaiah, Gamini Senanayake, Manickam Minakshi, Nanomaterials **7**, 356 (2017); https://doi.org/10.3390/nano7110356
[17] Ramesh Sivasamy, Potu Venugopal, Edgar Mosquera, Vacuum **175**, 109255 (2020); https://doi.org/10.1016/j.vacuum.2020.109255

[18] M.Manuraj, Jomiya Chacko, K.N.Narayanan Unni, R.B.Rakhi, J. Alloys Compd. **836**, 155420 (2020); https://doi.org/10.1016/j.jallcom.2020.155420
[19] W.A.Badawy, M.M. El-Rabiei, N.H.Helal, H.M.Nady, Z. Phys. Chem. **227**, 1143 (2013); https://doi.org/10.1524/zpch.2013.0347
[20] Zhe Tang, Chun-hua Tang, Hao Gong, Adv. Funct. Mater. **22**, 1272 (2012); https://doi.org/10.1002/adfm.201102796
[21] Weidong He, Chenggang Wang, Huiqiao Li, Xiaolong Deng, Xijin Xu, Tianyou Zhai, Adv. Energy Mater. **7**, 1700983 (2017); https://doi.org/10.1002/aenm.201700983
[22] Huanlei Wang, M.B.Chris, Holt, Zhi Li, Xuehai Tan, Babak Shalchi Amirkhiz, Zhanwei Xu, Brian, C. Olsen, Tyler Stephenson, David Mitlin, Nano Res. **5**, 605 (2012); http://dx.doi.org/10.1007/s12274-012-0246-x
[23] J.L.Boldú, R.J.Gleason, P.E.Muñoz, Rev. Mex. Fıs. **51,**199 (2005); http://www.redalyc.org/articulo.oa?id=57063813
[24] Sebastian Rast, Alain Borel, Lothar Helm, Elie Belorizky, Pascal H. Fries, Andre´ E. Merbach, J. Am. Chem. Soc.**123**, 2637 (2001); https://doi.org/10.1021/ja973427n
[25] Ram Kripal, Indrajeet Mishra, Physica B **405**, 425 (2010); https://doi.org/10.1016/j.physb.2009.08.305